ELSEVIER

Catalysis Today 30 (1996) 67-76

CATALYSIS TODAY

Constituent selection and performance characterization of catalysts for oxidative coupling of methane and oxidative dehydrogenation of ethane

Huilin Wan *, Zisheng Chao, Weizheng Weng, Xiaoping Zhou, Junxiu Cai, Khirui Tsai

Department of Chemistry and State Key Laboratory for Physical Chemistry of the Solid Surface, Xiamen University, Xiamen 361005, China

---

Abstract

The catalytic property of BaF_2-doped tetragonal LaOF catalysts for oxidative coupling of methane and oxidative dehydrogenation of ethane was evaluated in detail by independently varying the concentration of BaF_2 in the catalysts. The results indicate that addition of BaF_2 into the tetragonal LaOF significantly improves the catalytic performance of LaOF for both reactions, and the best results are observed over the BaF_2/LaOF catalysts with BaF_2 content of ca. 10 mol%. The XRD analysis of the fresh catalysts suggests that, for the catalysts with BaF_2 content less than 15 mol%, most of the Ba^{2+} ions together with the accompanying F^- and O^{2-} may be dispersed in the LaOF, forming a Ba^{2+}-doped LaOF phase in which some of the La^{3+} lattice points might be replaced by the less positively charged Ba^{2+}, leading to the formation of an F-center, anion vacancies or O^- species in the LaOF lattice which will be favorable to the adsorption and activation of O_2. The results of in situ Raman characterization of the surface dioxygen species over the LaOF and 10% BaF_2/LaOF catalysts suggest that the improvement of alkane conversions on a BaF_2-doped LaOF may be explained by the relative abundance of the dioxygen adspecies over the catalyst. While one of the possible reasons for the significant improvement of the selectivities may have resulted from the favorable effect of F^- ions for the isolation of the surface oxygen adspecies.

Keywords: Oxidative coupling of methane; Oxidative dehydrogenation of ethane; Alkaline-earth fluorides doped lanthanum oxyfluoride catalysts; Defective fluoride structure; Anionic vacancy; Raman spectroscopy

---

1. Introduction

Since the early work of Keller and Bhasin [1] on the oxidative coupling of methane (OCM), there has been an extensive effort throughout the world to develop an economically feasible catalytic process for converting methane to C_{2+} hydrocarbons. Many catalyst systems have been developed for this reaction and most of them contain the oxides with basic properties [2] such as the oxides of alkali metals, alkaline earth metals and lanthanides. However, it is now evident that oxidative coupling catalysts need not be strongly basic oxides [3]. Some experimental evidences have shown that there is no simple correlation between the catalyst basicity

---

[*] Corresponding author.

SSDI 0920-5861(95)00330-4

and OCM activity [4]. A complex relationship exists between surface acidity/basicity and the catalytic activity/selectivity, and surface basicity alone cannot control OCM catalytic properties [5]. Moreover, catalysts with strong basicity were easily poisoned by the CO_2 generated in the reaction, so that higher reaction temperature was required to maintain an adequate level of activity. Many investigators have found that the catalytic property, especially the selectivity to ethylene, can be significantly improved by chlorine present either in the form of a chloride component built into the catalyst or as a volatile chlorinated compound (organic or inorganic) in the reactant feed [2,6]. Recently, Lunsford et al. have reported a Cl^- promoted Li^+–MgO system which shows good catalytic performance for both OCM and ODE (oxidative dehydrogenation of ethane) [7,8]. Based on their studies, Lunsford suggested that the presence of Cl^- ions at an appropriate level modified the catalyst so that it no longer functioned as a strongly basic oxide catalyst and would not be easily poisoned by CO_2. Therefore, under steady-state conditions a less basic catalyst may be more active, particularly with respect to ODE, since ethane has a weaker C–H bond than methane.

In addition to chloride, it will also be interesting and of fundamental significance to have a detailed investigation on the influences of other halides, especially fluoride, on the catalytic properties of the OCM and ODE catalysts. The general reasons of considering fluoride first instead of bromide or iodide are as follows: (i) alkaline-earth and rare-earth fluorides are usually more stable than the corresponding chlorides, bromides or iodides, so the loss of fluorine during the OCM and ODE reactions may be less compared to the other halides; (ii) F^- ($r = 1.33$ Å) and O^{2-} ($r = 1.32$ Å) have similar ionic radii, and anionic exchange between metal fluoride and metal oxide may easily take place, leading to the formation of lattice defects, such as anionic vacancies that are requisites for the adsorption and activation of O_2 over compound catalysts with stable cationic valencies; (iii) the fluoride-doped OCM and ODE catalysts would be less basic than the undoped metal oxides, thus they will be favorable to the prevention of CO_2 inhibition as well as to the improvement of the catalytic activity; (iv) the distribution of F^- ions on the catalyst surface will have a positive effect on the dispersion of the surface active oxygen species that will be helpful to decrease the deep oxidation and improve the C_{2+} selectivity. Following these clues, a series of metal-fluoride promoted metal-oxide catalysts were developed, many of the catalysts demonstrated a satisfactory catalytic property for both OCM and ODE reactions [9–13]. XRD characterizations of the catalysts clearly indicated that anionic exchange did happen between the metal-oxide and the metal-fluoride phases, as have been proven by the observation of the lattice expansion/contraction of oxide/fluoride phases and the formation of the new oxyfluoride compounds in the catalysts containing rare earth elements as well as transition metals [9–13]. Among these oxyfluoride compounds, the LaOF phase has been identified in several catalysts prepared with LaF_3 as a starting material (followed by calcination which removes part of the F^-), including the LaF_3/SrO system that shows good catalytic property for OCM [12] and the LaF_3/BaF_2 system that is good for ODE [11,12]. As has been indicated in the literatures, LaOF has the fluorite-type structure or its superstructure [14,15], depending on the arrangement of the anions, it can form the stoichiometric rhombohedral phase (LaOF) as well as the nonstoichiometric tetragonal phase (expressed by the formula LaO_xF_{3-2x}, $0.7 < x < 1$) and cubic phases (observed in the LaOF–$La_4O_3F_6$ region) [15]. In the latter two cases, the excess of F^- ions occupy some of the interstitial positions as Frenkel defects. This result is consistent with the fact that many compounds with fluorite-like structure, such as alkaline-earth halides, ZrO_2 etc. contain anion Frenkel defects and anionic vacancies [16], and indicates that tetragonal or cubic LaOF is actually a compound with defective fluorite structure. It has been generally accepted that one of the essential conditions for a compound with stable cationic valency to be a good OCM catalyst is the presence and the mobility of the anionic vacancies in the lattice, so as to adsorb and activate O_2 during the reaction. Among the normally used OCM catalyst systems of oxide or composite-oxide, there is a series of catalysts with good catalytic performance in which the oxides of fluorite structure or defective fluorite structure, such as the cubic C-type structure, have been adopted as the hosts of catalysts [2,17,18]. Correspondingly, for the above mentioned fluoride-promoted OCM catalyst system, it is also possible to develop a new series of catalysts with good catalytic properties for oxidative dehydrogenation of light alkanes, in which LaOF of fluorite structure or its superstructure is employed as a fluoride-containing host. By proper doping of LaOF with metal fluorides of lower cationic valency such as alkaline-earth fluorides, it may be possible to create a LaOF of defective fluorite structure with higher concentration of anionic defects including F-centers and anionic vacancies, as a result, the catalytic properties of LaOF may also be improved.

In the present study, the catalytic properties of BaF_2-doped tetragonal LaOF catalyst for OCM and ODE reactions were evaluated in detail by independently varying the concentration of BaF_2 in the catalyst, with attention being given to the correlations between catalytic properties and the bulk composition and structure of the catalysts. The results of photocurrent measurement with LaOF or BaF_2/LaOF catalyst as a working electrode as well as ex situ and in situ Raman spectroscopic characterization of the oxygen species performed at 650°C, 550°C and 25°C over the LaOF and BaF_2/LaOF catalysts are presented. These results will provide us with more information for the understanding of the nature of the promotion effects of the F^- ions in metal fluoride/metal oxide system, especially for the catalyst system in which alkaline-earth fluoride or oxide is employed as the dopant of lanthanum oxyfluoride.

2. Experimental

LaOF was prepared by grinding equal molar ratios of LaF_3 and La_2O_3 in a mortar. The mixture was then pressed to pellets under a pressure of 300 kg/cm^2, followed by calcination at 900°C for 4 h. XRD measurement proved that the resulting material was tetragonal LaOF. BaF_2/LaOF catalysts were prepared by mixing appropriate amounts of BaF_2 and LaOF according to the same procedures used for LaOF preparation. After calcination at 800°C in air for 4 h, the pellets of LaOF and BaF_2/LaOF were crushed and sieved to grain size of 20 to 40 mesh.

The catalytic reactions were performed in a plug-flow fixed-bed quartz reactor (i.d. 0.80 cm) under atmospheric pressure. For OCM reaction, 0.50 ml of catalyst was loaded in the middle part of the reactor. For ODE reaction, 2.0 ml of catalyst was loaded in the middle part of the reactor and the rest of the reactor was filled with quartz sand of grain size of 20 to 40 mesh. No diluent gas was used in all reactions. A Shang Fen 102-GD gas-chromatograph (operated at room temperature) equipped with thermal conductivity detector was employed to analyze the gaseous effluent. A 5 Å molecular sieve column was used to analyze O_2, CO and CH_4 and a Porapak Q column to analyze CO_2, C_2H_4 and C_2H_6. The conversion of alkane (X_{alkane}) and selectivity (S_i) were calculated from the equations: $X_{alkane} = (\Sigma A_i \times F_i)/[\Sigma(A_i \times F_i) + A_{alkane} \times F_{alkane}]$ and $S_i = (A_i \times F_i)/\Sigma(A_i \times F_i)$, respectively, where A = peak area of carbon-containing species and F = correction factor of response and carbon number.

XRD analysis of the catalyst samples was carried out on a Rigaku Rotaflex D/max-C XRD system using Cu Kα(λ = 1.5406 Å) radiation. The specific surface area of the catalysts was measured by the BET method at liquid nitrogen temperature on a Sorpmatic-1900 system with N_2 as adsorbate.

Photocurrent measurement was carried out in

Table 1
The OCM performance of the $BaF_2/LaOF$ catalysts with different BaF_2 content [a]

Content of BaF_2 (mol%)	Conversion of CH_4 (%)	Selectivity (%)					Yield of C_2 (%)
		CO	CO_2	C_2H_4	C_2H_6	C_2	
LaOF	25.0	12.6	40.8	27.2	19.4	46.6	11.7
5% $BaF_2/LaOF$	26.4	4.7	38.6	31.9	24.8	56.7	15.0
7% $BaF_2/LaOF$	26.8	9.0	32.7	35.5	22.8	58.3	15.6
10% $BaF_2/LaOF$	28.7	3.1	29.6	44.7	22.6	67.3	19.3
10% $BaF_2/LaOF$ [b]	19.5	0	18.8	41.2	40.0	81.2	15.8
10% $BaF_2/LaOF$ [c]	16.5	0	15.5	23.5	61.0	84.5	13.9
15% $BaF_2/LaOF$	27.9	3.0	29.1	43.7	24.2	67.9	18.9
18% $BaF_2/LaOF$	27.4	8.2	27.9	40.3	23.6	63.9	17.5
20% $BaF_2/LaOF$	26.9	9.9	27.0	41.6	21.5	63.1	17.0
30% $BaF_2/LaOF$	23.8	12.8	28.0	39.0	20.2	59.2	14.1

[a] Reaction conditions: feed = $CH_4:O_2 = 4:1$, temperature = 780°C, GHSV = 15000 h^{-1}.
[b] Reaction conditions: feed = $CH_4:O_2 = 6:1$, temperature = 770°C.
[c] Reaction conditions: feed = $CH_4:O_2 = 9:1$, temperature = 770°C.

0.1 M NaF aqueous solution on a conventional three-electrode system, with Pt disk, SCE and LaOF or $BaF_2/LaOF$ as the counter, reference and working electrodes, respectively. The electrodes were arranged in an electrolytic cell with quartz window. A deuterium lamp (DLPS-3, 30W) was used as the light source. The monochromatic light modulated with a Parc Light Chopper Model 197 was illuminated to the working electrode through the quartz window and the potential of the cell was controlled by a Hokuto Denko Dual Potentiostat/Galvanostat HR101B. The photocurrent were amplified and recorded by a Parc 5206 two-phase lock-in analyzer.

The Raman spectra were recorded on a Jobin

Table 2
The ODE performance of $BaF_2/LaOF$ catalysts with different BaF_2 content [a]

Content of BaF_2 (mol%)	Temp. (°C)	X_{O_2} [b] (%)	Conv. of C_2H_6 (%)	Selectivity (%)				Yield of C_2H_4 (%)
				CO	CH_4	CO_2	C_2H_4	
Quartz sand	700	31.7	3.0	0	0	25.8	74.2	2.2
	720	30.2	5.2	0	0	20.7	79.3	4.1
LaOF	660	0	44.6	13.3	4.0	24.2	58.5	26.1
6% $BaF_2/LaOF$	660	0	54.7	10.3	3.6	17.1	69.0	37.7
8% $BaF_2/LaOF$	660	0	55.2	2.9	3.8	19.3	74.0	40.8
10% $BaF_2/LaOF$	660	0	57.8	8.4	4.3	17.6	70.7	40.9
10% $BaF_2/LaOF$ [c]	660	0	75.5	11.8	8.6	12.7	66.9	50.5
12% $BaF_2/LaOF$	660	0	50.2	8.1	3.1	20.3	68.5	34.4
14% $BaF_2/LaOF$	680	0	53.4	9.8	3.6	19.7	66.9	35.7
26% $BaF_2/LaOF$	660	0	52.4	9.3	3.5	20.8	66.4	34.8
30% $BaF_2/LaOF$	660	0	46.2	8.0	3.5	24.5	64.0	29.6
30% $BaF_2/LaOF$ [d]	640	0	80.8	8.7	8.8	11.7	70.8	57.2

[a] Reaction conditions: feed = $C_2H_6:O_2 = 67.7:32.3$; GHSV = 2700 h^{-1}.
[b] X_{O_2} = the molar percentage of O_2 in the effluent.
[c] GHSV = 6000 h^{-1}.
[d] GHSV = 11600 h^{-1}.

Yvon U-1000 Raman spectrometer at a resolution of 4 cm^{-1} using a self-designed in situ Raman cell which could be heated up to 750°C. The temperature of the cell was measured by a thermal couple mounted close to the sample. In the experiments, the sample was first thermally treated at 750°C under H_2 for 2 h to remove the surface carbonate residue, followed successively by purging with He at 750°C, and exposure to O_2 at same temperature. The O_2-treated sample was then cooled down gradually under O_2 atmosphere from 750°C to 25°C within a period of 3 h, and the Raman spectra were recorded at specified temperature, i.e. 650, 550 and 25°C, respectively during the cooling period. At each specified temperature point, temperature of the Raman cell was maintained constant for about 15 min to insure that the Raman measurement was conducted under thermostatic condition.

3. Results and discussion

3.1. Catalytic performance

The catalytic performance of the LaOF-based catalyst for OCM and ODE reactions are listed in Tables 1 and 2. The data for OCM and ODE were collected after 10 and 6 h on stream, respectively. It can be seen from Table 1 that LaOF is an active catalyst for OCM at 780°C, however, its selectivity for C_2 hydrocarbons was only about 46.6%. When 5 mol% of BaF_2 was added to the LaOF, the catalytic performance improved significantly. With the increase of BaF_2 content from 5 to 10 mol%, both CH_4 conversion and C_2 selectivities increased, and the highest CH_4 conversion and C_2 selectivity were obtained over the catalysts with BaF_2 contents of 10 to 15 mol%. The catalyst could run for about 100 h maintaining the C_2 yield at about 18 to 19%. Since OCM reaction is a strongly exothermic reaction, the management of the large amount of heat released has also attracted much attention. Generally, it may be acceptable to carry out the reaction at lower conversion of CH_4 and higher C_2 selectivity [3]. As shown in Table 1, the CH_4 conversion and C_2 selectivity over the BaF_2/LaOF catalyst could be controlled by varying the CH_4:O_2 ratio. When the CH_4:O_2 ratio increased to 6:1 and 9:1, C_2 selectivities of 81.2 and 84.6% with CH_4 conversions of 19.5 and 16.5% were obtained over 10%BaF_2/LaOF catalyst at 770°C.

As can be seen from Table 2, LaOF is also an active catalyst for ODE at 660°C, but its selectivity for ethylene formation is limited to 58.5%. When BaF_2 was added to LaOF, both ethane conversion and ethylene selectivity increased significantly, and the catalysts with BaF_2 content close to 10 mol% gave the highest ethane conversions and ethylene selectivities under the conditions of 660°C and GHSV = 2700 h^{-1}. Even higher ethane conversions can be obtained

Table 3
XRD analysis results of BaF_2, LaOF and BaF_2/LaOF catalysts

Samples (fresh catalyst)	d (Å) (I/I_0)									
BaF_2 (standard)	3.579(100)		3.100(27)		2.193(79)			1.870(51)		
LaOF (standard)		3.35(100)		2.90(25)		2.06(60)	2.05(33)		1.76(22)	1.75(44)
LaOF (prepared)		3.348(100)		2.892(18)		2.051(33)	2.044(24)		1.756(10)	1.743(34)
5% BaF_2/LaOF	3.534(5)	3.341(100)		2.840(16)		2.048(35)			1.752(11)	1.742(29)
10% BaF_2/LaOF	3.537(8)	3.346(99)		2.890(21)		2.051(39)	2.044(25)		1.755(10)	1.743(34)
15% BaF_2/LaOF	3.537(12)	3.346(100)		2.890(19)		2.051(38)	2.043(22)		1.753(9)	1.743(27)
18% BaF_2/LaOF	3.562(21)	3.346(99)		2.888(19)	2.178(12)	2.051(36)	2.044(23)	1.856(10)	1.755(9)	1.743(27)
20% BaF_2/LaOF	3.559(29)	3.348(100)	3.081(10)	2.890(20)	2.178(18)	2.052(35)	2.044(23)	1.857(11)	1.753(9)	1.743(26)
30% BaF_2/LaOF	3.565(45)	3.346(100)	3.087(11)	2.888(21)	2.178(27)	2.052(38)	2.044(23)	1.860(19)	1.753(10)	1.743(27)

at higher GHSV. However, there is no simple correlation between the ethylene selectivity and the GHSV which may indicate that a hot spot exists in the reactor, especially at higher GHSV. The life-span test with a 14% $BaF_2/LaOF$ catalyst showed no decrease in catalytic activity and ethylene selectivity during 26 h on stream. However, taking in consideration that the life time of the same catalyst for OCM was higher than 100 h, and that the reaction temperature of OED was much lower than that of OCM, it is expected that the catalyst will demonstrate even better stability for ODE reaction.

3.2. XRD and BET specific surface area measurement

The phase composition of LaOF and $BaF_2/LaOF$ with different BaF_2 content were determined by XRD, and the results were listed in Table 3. It can be seen that the tetragonal LaOF, which has a defective fluoride structure and can be expressed by the formula LaO_xF_{3-2x}, $(0.7 < x < 1)$ [14,15], were detected in the LaOF and $BaF_2/LaOF$ prepared with different BaF_2 contents. However, for the $BaF_2/LaOF$ with BaF_2 content less than 15%, XRD could hardly detect the BaF_2 phase, only the strongest diffraction line of BaF_2 with $d \approx 3.53$ could be found. These results suggest that when the BaF_2 content was 15 mol% or less, most of the BaF_2 was dispersed in the LaOF, forming a BaF_2- or BaO-containing LaOF phase. Under the circumstances, some of the La^{3+} lattice points might be replaced by the less positively charged Ba^{2+}, leading to the formation of F-centers, anionic vacancies or O^- species in the LaOF lattice to maintain electroneutrality. Comparing with the lattice of standard LaOF, the lattice of LaOF in the prepared samples (LaOF or $BaF_2/LaOF$) slightly contracted. A possible explanation for the phenomenon is that the latter one may contain higher concentrations of anionic vacancies. These vacancies may result from partial replacement of the F^- by O^{2-} ions due to slow hydrolysis of LaOF in the calcination process (for the cases of LaOF and $BaF_2/LaOF$) and partial substitution of the La^{3+} in the lattice by the Ba^{2+} ion (for the case of $BaF_2/LaOF$). When the content of BaF_2 was above 15 mol%, the LaOF lattice could not accommodate all the BaF_2, and thus a separate BaF_2 phase was formed. In this case, some of Ba^{2+} in the BaF_2 lattice might also be substituted by La^{3+}, leading to the formation of a lattice contracted BaF_2 phase taking in consideration the more positive charge and a smaller ionic size of La^{3+} than Ba^{2+}.

The data of the specific surface area of the catalysts were listed in Table 4. As shown in the Tables 1 and 2, the selectivities to C_2 (for OCM) or ethylene (for ODE) over $BaF_2/LaOF$ catalysts were higher than those over LaOF, while the specific surface area of the $BaF_2/LaOF$ catalyst was larger than that of LaOF. Thus the increase in the selectivities over $BaF_2/LaOF$ catalysts cannot be attributed to a reduction in surface area. It may result mainly from the isolation effect of the F^- ions to the surface oxygen adspecies as a result of dispersion and/or formation of the alkaline-earth fluorides on the surface of the $BaF_2/LaOF$ system.

3.3. Photocurrent measurement and Raman spectroscopic characterization of the oxygen adspecies over the LaOF and BaF_2/LaOF

The experiment of photocurrent measurement with LaOF or $BaF_2/LaOF$ as working electrode shows that, in the range of 0.30 to 1.0 V of

Table 4
The BET specific surface area of LaOF, BaF_2 and $BaF_2/LaOF$ catalysts

	BaF_2 content (mol%)										
	0	5.0	8.0	10.0	12.0	15.0	18.0	20.0	26.0	30.0	100
Specific surface area (m^2/g)	2.9	11.0	5.2	6.5	4.7	7.5	6.3	5.1	4.4	4.3	2.7

applied potentials, the cathodic and anodic photocurrents were detected on the LaOF and 10% BaF_2/LaOF electrodes, respectively, and the intensities of photocurrent in the latter system were found to be about 100 times as high as those in the former one (Fig. 1). These results suggest that LaOF is a solid electrolyte with 'p-type' conductivity, after modifying with 10% BaF_2, the conductivity of the sample changes to 'n-type', implying the possible formation of F-center or more anionic vacancies, or decrease of the concentration of interstitial F^- ions in the 10% BaF_2/LaOF system as the result of partial substitution of the La^{3+} in the LaOF lattice by Ba^{2+}. Incidentally, this result indicates that p-type conductivity may not be a requisite attribute for a good OCM catalysts.

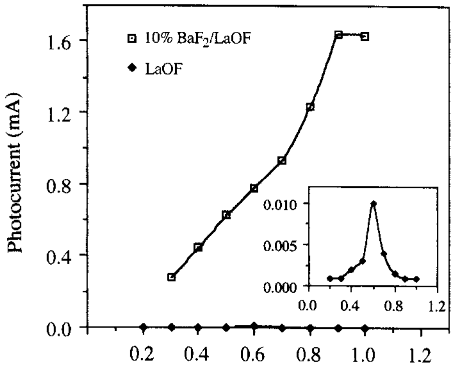

Fig. 1. Plots of photocurrent intensities vs. applied potentials. Cathodic and anodic currents were detected on the LaOF and BaF_2 /LaOF electrodes, respectively.

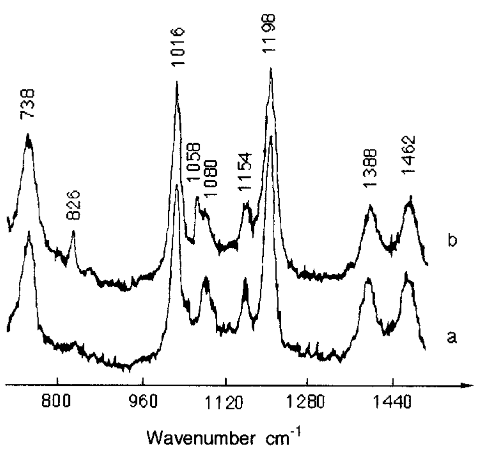

Fig. 2. Room temperature Raman spectra of the catalysts. (a) O_2 adsorbing 10% BaF_2 /LaOF. (b) After treatment of (a) with 1 atmosphere of CO_2 at 750°C followed by cooling to room temperature under CO_2.

The Raman spectroscopic characterizations of the oxygen adspecies under various temperatures were carried out over the LaOF and 10% BaF_2/LaOF catalysts. Fig. 2a shows the room temperature Raman spectrum of an O_2-treated 10% BaF_2/LaOF. Before the sample was exposed to O_2 at room temperature, it had been treated with H_2 at 750°C for 2 h followed by cooling down under He atmosphere. No Raman peak was observed in the region of 700–1500 cm^{-1} over the H_2 treated 10% BaF_2/LaOF before exposure to O_2. As can be seen in Fig. 2a, after exposure to O_2, several Raman peaks attributable to the surface dioxygen adspecies were observed in the wavenumber range of 738–1462 cm^{-1}. The peak at 738 cm^{-1} is close to the low end of the wavenumber region for the peroxide species, and may be assigned to the surface O_2^{2-} species [19]. The Raman peaks at 1016, 1042, 1080, 1154 and 1198 cm^{-1} are close to the known IR bands of adsorbed O_2^- (1015–1160 cm^{-1}) observed and attributed by Zecchina et al. [20] over the diluted MgO–CoO solid solution, based on the isotope substitution experiments and the comparison with homogeneous analogues, and that (1180 cm^{-1}) reported by Davydov et al. [21] on O_2-adsorbed TiO_2, and may tentatively be assigned to the surface O_2^- species with different adsorption modes in different chemical environments. In order to explain the IR peaks of surface O_2^- species with lower stretching frequencies, such as the peak at 1015 cm^{-1}, Zecchina et al. [20] have suggested a bridged μ-superoxo adsorption mode. This suggestion could actually be correlated to that proposed by Madix et al. [22] and Biloen et al. [23] in which low-frequency peroxide species on Ag(110) may have resulted from the possible increased donation from the O_2 π orbitals to the empty orbitals of the central metal besides the electron back-donation into the π^* orbitals of the oxygen molecule. The preliminary results of isotope substitution experiment performed on 20% $BaF_2/LaOF$ by Zhou et al. [24] indicated that, after exchanging with $^{18}O_2$, the peaks at 738 and 1198 cm^{-1} shifted to ca. 700 and 1126 cm^{-1}, respectively. The observed isotope shifts for these two peaks are in good agreement with theoretically expected values of the difference between the stretching frequencies of $^{16}O-^{16}O$ and $^{18}O-^{18}O$ species. The peaks at 1388 and 1462 cm^{-1} are lower than the frequency range of adsorbed neutral O_2 species (ca. 1550 cm^{-1}) but higher than that of the superoxide species, and can be assigned to the weakly adsorbed species ($O_2^{\delta-}$) between adsorbed O_2^- and O_2. In order to get rid of the possible interference of the surface carbonate species to the assignment of the oxygen adspecies, the CO_2 adsorption experiment was also performed. After the above O_2-treated 10% $BaF_2/LaOF$ was heated at 750°C under one atmosphere of CO_2 followed by cooling to room temperature under CO_2, the corresponding Raman spectrum is shown in Fig. 2b. As can be seen, in addition to the peaks of adsorbed dioxygen species, two bands at 826 and 1058 cm^{-1} with medium intensities were also observed. These bands obviously result from the surface carbonated species. Comparing with the Raman spectra of a working OCM catalysts of the composite metal-oxide type such as Th–La–O_x [25], the band intensity of the surface carbonate species over the 10% $BaF_2/LaOF$ is much lower, implying that basicity of the $BaF_2/LaOF$ system is much weaker compare to that of the oxide system. This property is important for an OCM or ODE catalyst to give a lower ‘light off’ temperature. The similar CO_2 adsorption experiment was also performed over the LaOF catalyst; however, the peaks of surface carbonate species were hardly detectable, a possible explanation is that the surface of the LaOF is less basic than the BaF_2 doped LaOF, leading to decreased adsorption of CO_2 on LaOF.

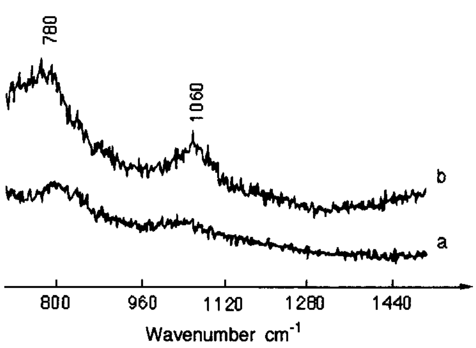

Fig. 4. Raman spectra of (a) LaOF and (b) 10% BaF_2 /LaOF after exposure to O_2 at 750°C followed by cooling to 550°C under O_2.

Figs. 3–5 show the in situ and ex situ Raman spectra of oxygen adspecies on LaOF (a) and 10% $BaF_2/LaOF$ (b) recorded at 650, 550 and 25°C, respectively, during the period when the samples were cooling from 750°C to room temperature under O_2 atmosphere. Before the samples were exposed to O_2 at 750°C, similar treatment procedures as above were also followed in

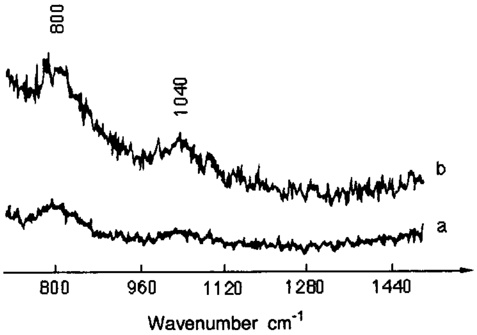

Fig. 3. Raman spectra of (a) LaOF and (b) 10% BaF_2 /LaOF after exposure to O_2 at 750°C followed by cooling to 650°C under O_2.

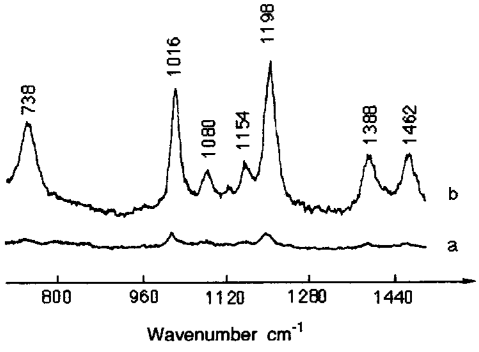

Fig. 5. Raman spectra of (a) LaOF and (b) 10% BaF_2 /LaOF after exposure to O_2 at 750°C followed by cooling to room temperature under O_2.

order to clean the surface. As shown in Figs. 3 and 4, the Raman spectra recorded at 650°C and 550°C were not well resolved. Two broad bands with maxima at ca. 780–800 cm^{-1} and 1040–1060 cm^{-1}, respectively, can be identified, and the intensity of the bands at 550°C was a little higher than that at 650°C. The bands with maxima at ca. 800 cm^{-1} (LaOF) and 780 cm^{-1} (BaF_2/LaOF) were closed to the frequencies of peroxide signal, and might be assigned to the adsorbed O_2^{2-} species [19]. The Raman signals of surface peroxide species over La_2O_3, Na^+ or Sr^{2+} modified La_2O_3 and Ba^{2+}/MgO with frequencies between 823 and 878 cm^{-1} have been observed by Knozinger and Lunsford et al. at 700°C [3,26]. Based on the above discussion, the bands centered at ca. 1050 cm^{-1} may be attributed to the O_2^- adspecies [20]. Comparatively, the spectrum recorded at room temperature (Fig. 5) are much better resolved, and it shows exactly the same peaks as we have seen in Fig. 2a. As can be seen, the surface carbonate peaks at 828 and 1058 cm^{-1} are not observed in Fig. 5, indicating that the possibility of coexistence of the surface carbonate species with the adsorbed dioxygen species in Figs. 3 and 4 can be excluded or beyond the detection limit of Raman spectroscopy. It is also clear to see from Figs. 3–5 that intensities of bands of the oxygen adspecies (O_2^{2-} and O_2^-) over the 10% BaF_2/LaOF are significantly higher than those over the LaOF. This accounts for the improvement of the alkane conversion over the Ba^{2+} doped LaOF catalysts, and the increase in the surface concentration of oxygen adspecies (O_2^{2-} and O_2^-) may also be explained by the possible formation of F-centers or higher concentration of anionic vacancies in the BaF_2/LaOF system compared with the LaOF system.

4. Conclusions

Based on the above results, we may conclude that addition of BaF_2 into the tetragonal LaOF significantly improves the catalytic performance of LaOF for both OCM and ODE. The best results were observed over the BaF_2/LaOF catalysts with BaF_2 content of ca. 10 mol%. Under this condition, most of the Ba^{2+} ions together with the accompanying F^- and O^{2-} may be dispersed in the LaOF, forming a Ba^{2+}-doped LaOF phase in which some of the La^{3+} lattice points might be replaced by the less positively charged Ba^{2+}, leading to the formation of F-centers, anion vacancies or O^- species in the LaOF lattice which will be favorable to the adsorption and activation of O_2. The results of in situ Raman characterization of the surface dioxygen species over the LaOF and 10% BaF_2/LaOF catalysts suggest that the improvement of alkane conversions on a BaF_2 doped LaOF may be explained by the relative abundance of the dioxygen adspecies over the catalyst. While one of the possible reasons for the significant improvement of the selectivities may have resulted from the favorable effect of F^- ions for the isolation of the surface oxygen adspecies. Though hydrolytic loss of F^- from such catalyst system was detected by analysis, this type of catalyst may still be promising especially as catalyst operating for ODE at lower temperature (600°C). The studies of this type of catalysts illustrate many important points on the activity/selectivity/stability controlling factors of OCM and ODE catalysts.

Acknowledgements

This Work is supported by the National Natural Science Foundation of China.

References

[1] G.E. Keller and M.M. Bhasin, J. Catal., 73 (1982) 9.
[2] A.M. Maitra, Appl. Catal. A: Gen., 104 (1993) 11.
[3] J.H. Lunsford, in H.E. Curry-Hyde and R.F. Howe, Nature Gas Conversion II, Elsevier Science, 1994, p. 1.
[4] J.A. Lapszewicz and X.Z. Jiang, Catal. Lett., 13 (1992) 103.
[5] V.R. Choudhary and V.H. Rane, J. Catal., 130 (1991) 411.
[6] O.V. Krylov, Catal. Today, 18 (1993) 209.

[7] J.H. Lunsford, P.G. Hinson, M.P. Rosynek, C. Shi, M. Xu and X. Yang, J. Catal., 147 (1994) 301.

[8] D. Wang, M.P. Rosynek and J.H. Lunsford, J. Catal., 151 (1995) 155.

[9] S. Zhou, X. Zhou, H. Wan and K.R. Tsai, Catal. Lett., 20 (1993) 179.

[10] X. Zhou, W. Zhang, H. Wan and K. Tsai, Catal. Lett., 21 (1993) 113.

[11] X.P. Zhou, S.Q. Zhou, F.C. Xu, S.J. Wang, W.Z. Weng, H.L. Wan and K.R. Tsai, Chem. Res. Chin. Univ., 9(3) (1993) 269.

[12] X.P. Zhou, S.Q. Zhou, W.D. Zhang, Z.S. Chao, W.Z. Weng, R.Q. Long, D.L. Tang, H.Y. Wang, S.J. Wang, J.X. Cai, H.L. Wan and K.R. Tsai, Preprints, Div. Petro. Chem. Inc., 39(2) (1994) 222.

[13] X.P. Zhou, Z.S. Chao, W.Z. Weng, W.D. Zhang, S.J. Wang, H.L. Wan and K.R. Tsai, Catal. Lett., 29 (1994) 177.

[14] A.F. Wells, Structural Inorganic Chemistry, 5th edn., Clarendon Press, Oxford, 1984, pp. 252, 482.

[15] K. Niihara and S. Yajima, Bull. Chem. Soc. Jpn., 44 (1971) 643.

[16] Z. Zhang, X. Verykios and M. Baerns, Catal. Rev., Sci. Eng., 36(3) (1994) 507.

[17] Y. Amenomiya, V.I. Birss, M. Goledzinowski, J. Galuszka and A.R. Sanger, Catal. Rev. Sci. Eng., 32 (1990) 163.

[18] Y.D. Liu, G.D. Lin, H.B. Zhang, J.X. Cai, H.L. Wan and K.R. Tsai, Preprints, Fuel Chem. Div., 37(1) (1992) 356.

[19] M. Che and A.J. Tench, Adv. Catal., 33 (1983) 1.

[20] A. Zecchina, G. Spoto and S. Coluccia, J. Mol. Catal., 14 (1982) 351.

[21] A.A. Davydov, M.P. Komarova, V.F. Anufrienko, N.G. Maksimov, Kinet. Katal., 14 (1973) 1519.

[22] B.A. Sexton and R.J. Madix, Chem. Phys. Lett., 76(2) (1980) 294.

[23] C. Backx, C.P.M. De Groot and P. Biloen, Surf. Sci., 104 (1981) 300.

[24] X.P. Zhou and C.T. Au, unpublished results.

[25] Y.D. Liu, H.B. Zhang, G.D. Lin, Y.Y. Liao and K.R. Tsai, J. Chem. Soc., Chem. Commun., (1994) 1871.

[26] G. Mestl, H. Knozinger and J.H. Lunsford, Ber. Bunsenges. Phys. Chem., 97 (3) (1993) 319.